THE ASTROPHYSICAL JOURNAL, 281: 9–12, 1984 June 1

SELF-SIMILAR SPHERICAL VOIDS IN AN EXPANDING UNIVERSE[1]

JAMES A. FILLMORE AND PETER GOLDREICH
California Institute of Technology
Received 1983 October 24; accepted 1983 December 5

ABSTRACT

We derive similarity solutions which describe the evolution of spherically symmetric voids in a perturbed Einstein–de Sitter universe filled with cold, collisionless matter. The character of a solution depends upon the profile of the initial density deficit. Gradual perturbations give rise to holes within which the density rises smoothly to the background value. Steep perturbations result in voids bounded by overdense shells with sharp edges, i.e., collisionless gravitational shocks.

Subject headings: cosmology — relativity

I. INTRODUCTION

The existence of large voids in the density of galaxies is a major new discovery of observational cosmology (Davis *et al.* 1982; Kirshner *et al.* 1981). Spherically symmetric numerical simulations (Peebles 1982; Hoffman, Salpeter, and Wasserman 1983; Hausman, Olson, and Roth 1983) and analytic fluid dynamical calculations (Sato 1982; Maeda, Sasaki, and Sato 1983; Sato and Maeda 1983) have been applied to demonstrate that empty holes may evolve from initial perturbations of slightly subcritical density. Similar voids commonly appear in three-dimensional N-body simulations (Klypin and Shandarin 1983; Frenk, White, and Davis 1983; Centrella and Melott 1983). Some of these simulations produced voids surrounded by dense shells. This suggests that planar superclusters may have formed from the fragmentation of shells which developed about initial perturbations of subcritical density, as well as from the collapse of initial perturbations of supercritical density. Our contribution is the derivation of similarity solutions for voids which display many of the features seen in the numerical simulations. This work is a sequel to Fillmore and Goldreich (1984, hereafter Paper I), which treated similarity solutions describing gravitational collapse.

The plan of the paper is as follows. In § II we study the early development of subcritical density perturbations. The similarity equation is derived in § III. Results obtained from the integration of this equation are presented in § IV.

II. EARLY DEVELOPMENT

As the scale of the perturbations which we are investigating is small compared with that of the horizon, Newtonian cosmology is an adequate approximation (Peebles 1980). For spherical symmetry, the equation of motion of a test particle reads

$$\frac{d^2r}{dt^2} = -\frac{4\pi G M(r, t)}{r^2}, \tag{1}$$

where $M(r, t)$ is the mass per unit solid angle within radius r at time t. The nonstandard definition of M follows Paper I.

We choose initial conditions such that at time t_i the unperturbed Hubble law

$$\frac{dr}{dt} = \frac{2}{3}\frac{r}{t} \tag{2}$$

is exactly satisfied. The initial position of a test particle is denoted either by its initial distance from the center r_i or by the initial mass between it and the origin, $M_i \equiv M(r_i, t_i)$.

Similarity solutions arise from scale-free initial perturbations. We take the initial perturbation mass $\delta M_i(M_i)$ to have the form

$$\delta \equiv \frac{\delta M_i}{M_i} = -\left(\frac{M_i}{M_0}\right)^{-\epsilon}, \quad \delta < 0, \tag{3}$$

where M_0 is a reference mass; the corresponding reference radius is r_0. The parameter ϵ, which determines the steepness of the initial mass deficit, must lie between zero and unity in order that the initial mass perturbation increase and the initial density perturbation decrease away from the origin.

The initial conditions require some comment; clearly, they are not physically reasonable for $r_i < r_0$, where they imply negative initial mass. We imagine that they pertain only in the region of small $|\delta|$. It is then a plausible but unproven conjecture that they give rise to self-similar solutions at large times, $t \gg t_i$.

So long as a particle does not cross the trajectories of other particles, which we refer to as orbit crossing, its interior mass remains constant, and equation (1) may be integrated to determine $t(r)$. To first order in $|\delta| \ll 1$, we find

$$t = \frac{3t_i}{2|\delta|^{3/2}} \int_0^{r/(r_i|\delta|)} \frac{u^{1/2}du}{(1+u)^{1/2}}. \tag{4}$$

The form of equation (4) suggests that we adopt scaled time and radius variables τ and λ defined by

$$\tau \equiv \frac{t}{t_*} = \frac{4t}{3\pi t_i}|\delta|^{3/2}, \tag{5}$$

$$\lambda \equiv \frac{r}{r_*} = \frac{r|\delta|}{r_i}. \tag{6}$$

Although the powers of δ which appear in the scalings are uniquely determined, the multiplicative constants are arbitrarily chosen to be those taken in Paper I. However, they do not have the special significance that they did in Paper I, where $\tau = \lambda = 1$ corresponded to the unique event of turnaround. The trajectories of particles involved in the evolution of a void are not marked by an event of comparable significance; all choices of multiplicative constants are equally good.

Our choice of scaling defines a fiducial radius $R(t)$ and a

[1] Contribution No. 4004 of the Division of Geological and Planetary Sciences, California Institute of Technology.

corresponding initial mass M_t which are associated with particles whose $t_* = t$. From equations (3) and (5), it follows that

$$R(t) = r_0 \lambda(1)\left(\frac{4t}{3\pi t_i}\right)^{2/3 + 2/(9\epsilon)}, \tag{7}$$

$$M_t = M_0\left(\frac{4t}{3\pi t_i}\right)^{2/(3\epsilon)}. \tag{8}$$

The factor

$$\lambda(1) \approx 2.3236 \tag{9}$$

is obtained by evaluating the integral in equation (4) for $\tau = 1$.

The study of equation (4) reveals that orbit crossing occurs only for $\epsilon > \frac{2}{3}$. Thus, equation (4) is valid for all t if $\epsilon < \frac{2}{3}$. The distinction between $\epsilon < \frac{2}{3}$ and $\epsilon > \frac{2}{3}$ may be understood by noticing that the particle terminal velocity, computed neglecting orbit crossing, is an increasing function of M for $\epsilon < \frac{2}{3}$ and a decreasing function of M for $\epsilon > \frac{2}{3}$. A similar argument was given by Sato (1982).

Proper application of Newtonian cosmology requires that the linear dimensions of the structures be small compared with the distance to the horizon. This restricts the interval of time over which the similarity solutions with $\epsilon < \frac{2}{3}$ are valid because their fiducial radii grow faster than t.

III. DERIVATION OF SIMILARITY EQUATION

As the derivation of the similarity equation parallels that given in Paper I, we omit many details. The major step is to express $M(r, t)$ as a functional of λ. We appeal to self-similarity and write

$$M(r, t) = M_t \mathcal{M}(r/R), \tag{10}$$

where $\mathcal{M}$ is the dimensionless mass profile function given by

$$\mathcal{M}\left(\frac{r}{R}\right) = \int_0^\infty \frac{dM_i'}{M_t} H[r(t; M_i) - r(t; M_i')]. \tag{11}$$

Here $H[u]$ is the Heaviside function; $H[u] = 1$ for $u \geq 0$, and $H[u] = 0$ for $u < 0$. Changing the variable of integration from M_i to τ with the help of equation (8) yields

$$\mathcal{M}\left(\frac{\lambda}{\Lambda}\right) = \frac{2}{3\epsilon}\int_0^\infty \frac{d\xi}{\xi^{1 + 2/(3\epsilon)}} H\left[\frac{\lambda}{\Lambda} - \frac{\lambda(\xi)}{\Lambda(\xi)}\right], \tag{12}$$

where

$$\Lambda \equiv \lambda(1)\tau^{2/3 + 2/(9\epsilon)} \tag{13}$$

has been defined such that

$$\frac{r}{R(t)} = \frac{\lambda}{\Lambda(\tau)}. \tag{14}$$

The integrals in equations (11) and (12) each differ in one boundary value from their counterparts in Paper I. The upper limit on the former and the lower limit on the latter are ∞ and 0; the corresponding values were M_t and 1 in Paper I. These changes are necessary because orbit crossing occurs before $\tau = 1$ for $\epsilon > 0.92$.

We use equations (5), (6), and (14) to rewrite the equation of motion (1) in terms of the scaled variables:

$$\frac{d^2\lambda}{d\tau^2} = -\frac{\pi^2}{8}\frac{\tau^{2/(3\epsilon)}}{\lambda^2}\mathcal{M}\left(\frac{\lambda}{\Lambda}\right). \tag{15}$$

Equation (15) governs the evolution of the similarity solutions for all values of τ. It is identical to the equation we used to compute spherically symmetric collapse solutions in Paper I. However, new boundary conditions are needed to obtain void solutions. These are obtained from equation (4) using the definitions given by equations (5) and (6). In principle, any pair (τ, λ) which satisfies equation (4) and precedes the first orbit crossing event is suitable. In practice, we use

$$\tau = 1, \quad \lambda = 2.3236, \quad \frac{d\lambda}{d\tau} = 1.8786 \tag{16}$$

for all of the examples shown in this paper. There is, however, a minor technical complication. For $\epsilon > 0.92$, orbit crossing takes place before $\tau = 1$; for $\epsilon = 1$, it occurs at $\tau \approx 0.6$. In treating these cases, the boundary conditions must be set at smaller values of τ.

IV. RESULTS

a) $\epsilon < \frac{2}{3}$

Since orbit crossing does not occur for this range of ϵ, the solution is given for all time by equation (4). The density profile is found from

$$\frac{\rho(r/R, t)}{\rho_b(t)} = \frac{3\pi^2}{16\epsilon\tau^{2/(3\epsilon)}}\left[\frac{R}{\lambda(1)r}\right]^3\left[\frac{1 + 3\epsilon}{3\epsilon} - \frac{3\pi\tau}{4}\frac{(1 + \lambda)^{1/2}}{\lambda^{3/2}}\right]^{-1}, \tag{17}$$

with the help of equations (4), (5), (6), (13), and (14), which implicitly determine τ and λ as functions of r/R. Here the background density $\rho_b(t) = (6\pi G t^2)^{-1}$.

Density profiles for two values of ϵ are displayed in Figure 1. The density increases monotonically with radius and gradually approaches the background value. Since $R(t)$ grows faster than t, each particle asymptotically approaches the center of the hole.

b) $\epsilon > \frac{2}{3}$

i) *Numerical Integrations*

The similarity solutions are obtained by numerical integration of the second-order differential equation (15) subject to the boundary conditions given by equation (16). Because the inte-

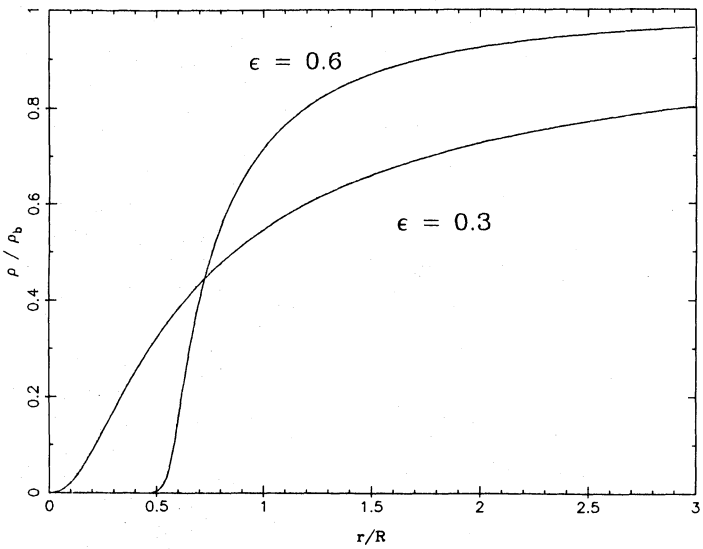

FIG. 1.—Ratio of actual to background density for $\epsilon = 0.3$ and 0.6

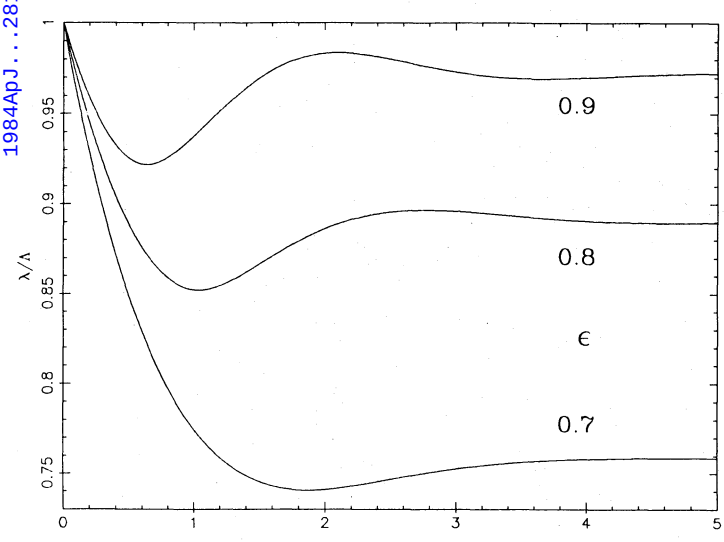

FIG. 2

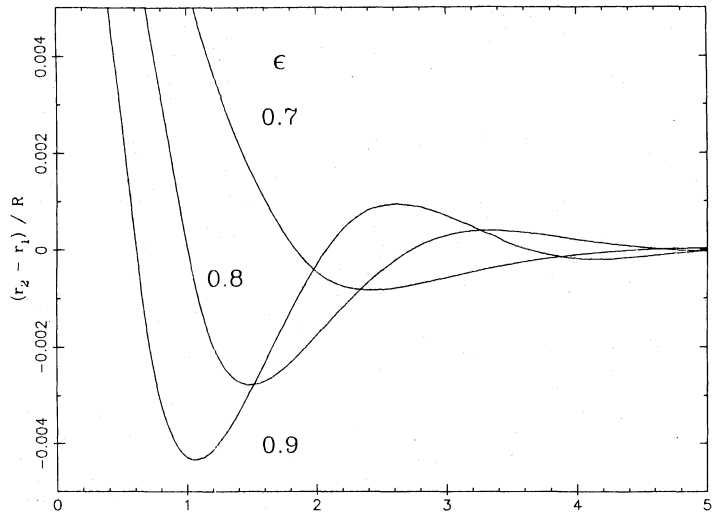

FIG. 3

FIG. 2.—Particle position relative to fiducial distance Λ for $\epsilon = 0.7, 0.8$, and 0.9

FIG. 3.—Difference in position of two nearby particles relative to the fiducial radius for $\epsilon = 0.7, 0.8$, and 0.9

gration must be carried out to very large values of τ, the independent variable is transformed from τ to $v = \ln(\tau)$, and λ is computed on a linear grid in v. Following an initial guess for $\mathcal{M}$, we alternately integrate equation (15) and then update $\mathcal{M}$ by using equation (12). This procedure is continued until the desired level of convergence is obtained.

Plots of λ versus τ are uninteresting, so we do not present any here; particle radii just increase monotonically with time. The variations of λ/Λ drawn in Figure 2 show oscillations of the particle radii scaled to the fiducial radii. Still more revealing are the plots in Figure 3, which illustrate the multiple crossings of neighboring orbits. From a comparison of Figures 2 and 3, it is seen that these crossings coincide with the maxima and minima of λ/Λ.

The orbit crossings have dramatic consequences. The density profiles displayed in Figure 4 all show completely empty holes surrounded by overdense shells. The density is infinite at the inner and outer shell boundaries, but these regions contribute negligibly to the surface density, as can be seen from the mass profiles plotted in Figure 5. The infinite-density spikes are truncated in the figures because the density is averaged over bins.

How does orbit crossing give rise to these structures, especially the sharp edges? Orbit crossing proceeds from the inside out; each particle is passed by all particles of smaller initial radii before passing its immediate outer neighbor. A particle begins orbit crossing when it is overtaken by the outer boundary of the shell. At this time it crosses the orbits of particles with significantly smaller initial radii. The first crossing of orbits of its original neighbors occurs when it reaches the inner

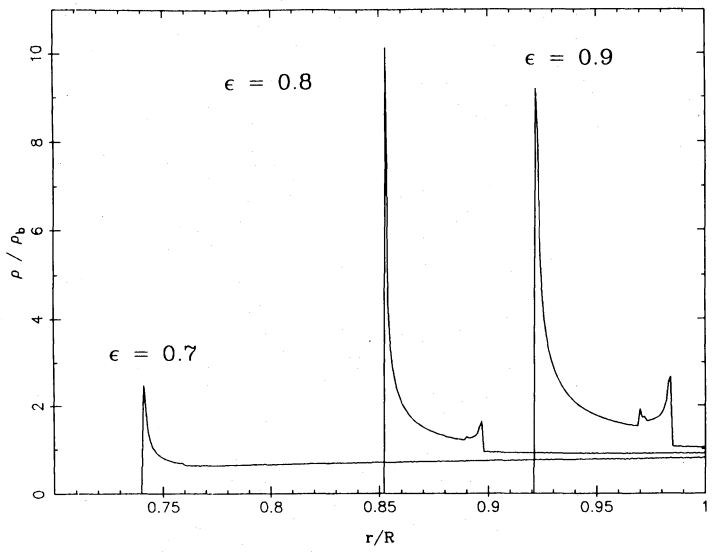

FIG. 4.—Ratio of actual to background density

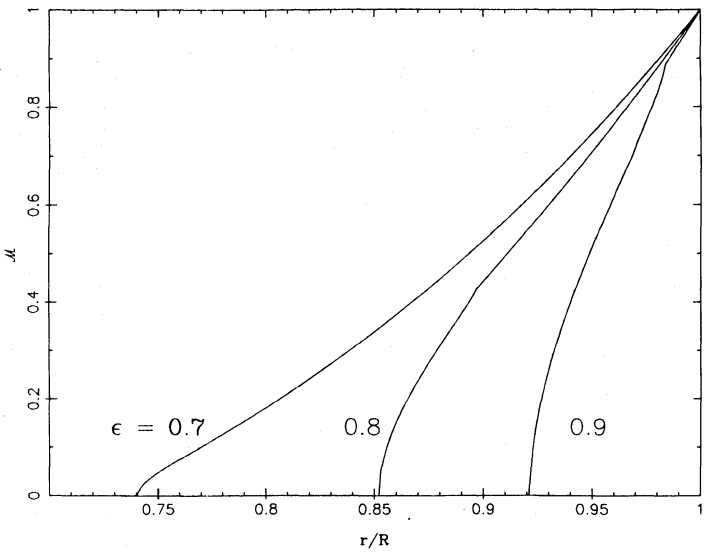

FIG. 5.—Profile of mass per unit solid angle

boundary of the shell. The inner and outer shell edges and other weaker density spikes within the shells are composed of particles which are in the act of crossing their neighbors' orbits.

ii) *Infall Velocity*

Peebles (1982) noted that particles in the shell surrounding a void do not have large streaming velocities. Thus, fragmentation of dense shells surrounding voids might produce planar structures having smaller peculiar velocities than those resulting from planar collapse of regions with supercritical density. This may be quantified by calculating the ratio of the infall velocity to the unperturbed Hubble velocity for both types of planar structures.

The peculiar velocity of a particle crossing the shell around a void for the first time is

$$v_i = \frac{dr}{dt} - f\frac{dR}{dt} = \frac{R(t)}{t}\left[\frac{\tau^{1/3-2/(9\epsilon)}}{\lambda(1)}\frac{d\lambda}{d\tau} - \frac{2f(1+3\epsilon)}{9\epsilon}\right], \quad (18)$$

where f is the ratio of the void's radius to $R(t)$. The Hubble velocity across the void's radius is

$$v_H = HfR = \frac{2f}{3}\frac{R(t)}{t}, \quad (19)$$

where H is the Hubble constant. The ratio of these velocities is

$$\frac{v_i}{v_H} = \frac{3\tau^{1/3-2/(9\epsilon)}}{2f\lambda(1)}\frac{d\lambda}{d\tau} - \left(1+\frac{1}{3\epsilon}\right). \quad (20)$$

For $0.7 \leq \epsilon \leq 1.0$, we find

$$0.05 \leq \frac{v_i}{v_H} \leq 0.15 .$$

For planar collapse (see Paper I), the infall velocity can be computed approximately by assuming the column density remains constant while a sheet falls toward the symmetry plane. Actually, the column density decreases because a sheet passes through previously collapsed material; however, this effect decreases the infall velocity by less than 15%. The desired velocity ratio is

$$\frac{v_i}{HZ} = 2^{1-1/\epsilon}, \quad (21)$$

where Z is the turnaround distance. The ratio in equation (21) varies from 0 to 1 as ϵ varies from 0 to 1, but it is greater than 0.15 for ϵ above 0.26.

iii) *Particle Motion in the Shell*

The damped oscillations in λ/Λ pictured in Figure 2 are easily modeled analytically. We transform the dependent variable in equation (15) from λ to $\zeta \equiv \lambda/\Lambda$. The equilibrium position, ζ_0, is given by

$$\frac{8\lambda(1)^3}{\pi^2} b\zeta_0^3 = \mathcal{M}(\zeta_0), \quad (22)$$

where

$$b = \left(\frac{2}{3}+\frac{2}{9\epsilon}\right)\left(\frac{1}{3}-\frac{2}{9\epsilon}\right).$$

The mean density interior to the equilibrium point is

$$\frac{\langle\rho(\zeta_0, t)\rangle}{\rho_b(t)} = \frac{9b}{2} \leq \frac{4}{9}. \quad (23)$$

Linearizing the equation of motion in terms of the variable $y = \zeta - \zeta_0$, we arrive at

$$\frac{d^2y}{d\tau^2} = -\frac{2}{\tau}\left(\frac{2}{3}+\frac{2}{9\epsilon}\right)\frac{dy}{d\tau} - \left[\frac{\pi^3}{2\lambda(1)^3}\frac{\rho(\zeta_0)}{\rho_b} - 3b\right]\frac{y}{\tau^2}. \quad (24)$$

Equation (24) is homogeneous in τ and has the solution

$$y = y_0\,\tau^{-\alpha}\cos\left[\beta \ln(\tau)\right], \quad (25)$$

where

$$\alpha = \left(\frac{1}{6}+\frac{2}{9\epsilon}\right), \quad \beta = \left[\frac{\pi^3\rho(\zeta_0)}{2\lambda(1)^3\rho_b} - 3b - \alpha^2\right]^{1/2}. \quad (26)$$

The oscillation period is proportional to τ as a consequence of the τ^{-2} variation of the density. As ϵ increases from 0.7 to 1.0, α decreases from 0.48 to 0.39, and β increases from 0.55 to 0.91.

J. A. F. would like to thank James Binney for a helpful discussion. Support for this research was provided by the National Science Foundation through a graduate fellowship to J. A. F. and through grant 80-20005.

REFERENCES

Centrella, J., and Melott, A. L. 1983, *Nature*, **305**, 196.
Davis, M., Huchra, J., Latham, D. W., and Tonry, J. 1982, *Ap. J.*, **253**, 423.
Fillmore, J. A., and Goldreich, P. 1984, *Ap. J.*, **281**, 1 (Paper I).
Frenk, C. S., White, S. D. M., and Davis, M. 1983, *Ap. J.*, **271**, 417.
Hausman, M. A., Olson, D. W., and Roth, B. D. 1983, *Ap. J.*, **270**, 351.
Hoffman, G. L., Salpeter, E. E., and Wasserman, I. 1983, *Ap. J.*, **268**, 527.
Kirshner, R., Oemler, A., Jr., Schechter, P., and Shectman, S. 1981, *Ap. J. (Letters)*, **248**, L57.
Klypin, A. A., and Shandarin, S. F. 1983, *M.N.R.A.S.*, **204**, 891.
Maeda, K., Sasaki, M., and Sato, H. 1983, *Progr. Theor. Phys.*, **69**, 89.
Peebles, J. E. 1980, *The Large-Scale Structure of the Universe* (Princeton: Princeton University Press), §§ 6–8.
———. 1982, *Ap. J.*, **257**, 438.
Sato, H. 1982, *Progr. Theor. Phys.*, **68**, 236.
Sato, H., and Maeda, K. 1983, *Progr. Theor. Phys.*, **70**, 119.

J. A. FILLMORE: Robinson 105-24, Caltech, Pasadena, CA 91125

P. GOLDREICH: 170-25 So. Mudd, Caltech, Pasadena, CA 91125